Blocking CXCR4-Mediated Cyclic AMP Suppression Inhibits Brain Tumor Growth *In vivo*

Lihua Yang,[1] Erin Jackson,[6] B. Mark Woerner,[1] Arie Perry,[2] David Piwnica-Worms,[3,6] and Joshua B. Rubin[1,4,5]

Departments of [1]Pediatrics, [2]Pathology and Immunology, [3]Molecular Biology and Pharmacology, [4]Anatomy and Neurobiology, and [5]Neurology and [6]Molecular Imaging Center, Mallinckrodt Institute of Radiology, Washington University School of Medicine and St. Louis Children's Hospital, St. Louis, Missouri

Abstract

The chemokine CXCL12 and its cognate receptor CXCR4 regulate malignant brain tumor growth and are potential chemotherapeutic targets. However, the molecular basis for CXCL12-induced tumor growth remains unclear, and the optimal approach to inhibiting CXCR4 function in cancer is unknown. To develop such a therapeutic approach, we investigated the signaling pathways critical for CXCL12 function in normal and malignant cells. We discovered that CXCL12-dependent tumor growth is dependent upon sustained inhibition of cyclic AMP (cAMP) production, and that the antitumor activity of the specific CXCR4 antagonist AMD 3465 is associated with blocking cAMP suppression. Consistent with these findings, we show that pharmacologic elevation of cAMP with the phosphodiesterase inhibitor Rolipram suppresses tumor cell growth *in vitro* and, upon oral administration, inhibits intracranial growth in xenograft models of malignant brain tumors with comparable efficacy to AMD 3465. These data indicate that the clinical evaluation of phosphodiesterase inhibitors in the treatment of patients with brain tumors is warranted. [Cancer Res 2007;67(2):651–8]

Introduction

Nearly 30 years ago, it was observed that higher grades of human brain tumors were associated with lower total adenylyl cyclase activity and decreased tumor cell cyclic AMP (cAMP; refs. 1, 2). It is now known that increased cAMP inhibits proliferation under most circumstances (3–6) and can also stimulate apoptosis (7–9). Thus, these earlier observations warrant re-evaluation as we search for therapeutic targets in our efforts to improve the outcome for patients with malignant brain tumors.

Decreased adenylyl cyclase activity and decreased intracellular cAMP could be the result of decreased adenylyl cyclase expression or decreased adenylyl cyclase activation. With respect to the latter, the expression of CXCR4 in malignant brain tumors is of particular interest. CXCR4 is a $G\alpha_i$-coupled chemokine receptor and therefore has the capacity to inhibit adenylyl cyclase activity and decrease intracellular cAMP (10–13). We and others have studied the expression and actions of CXCR4 in both neural and astrocytic brain tumors and found that CXCR4 can stimulate tumor growth and spread (11, 12, 14). We found that systemic delivery of AMD 3100, a small-molecule antagonist of ligand-induced activation of CXCR4, blocked the i.c. growth of both glioblastoma and medulloblastoma xenografts (12). These studies validated CXCR4 as a therapeutic target for the treatment of malignant brain tumors, but they did not identify the critical intracellular events that underlie CXCR4-dependent brain tumor growth, or the intracellular pathways that are targeted by AMD 3100 action.

More recently, we developed a novel phospho-specific antibody that recognizes a ligand-induced form of CXCR4 and showed that increased grade of astrocytoma is associated with increased CXCR4 phosphorylation (13). Activation of CXCR4 would be predicted to inhibit adenylyl cyclase and decrease intracellular levels of cAMP (15). Thus, the association between increased tumor grade and ligand-activation of CXCR4 could mechanistically link the earlier observations that cAMP levels are negatively correlated with the degree of malignancy in brain tumors.

Here, we report that cAMP suppression is key to CXCR4-mediated brain tumor growth, and that the antitumor effect of the CXCR4 antagonist AMD 3465 can be accounted for by its ability to block CXCL12-induced cAMP suppression. Furthermore, this antitumor effect is mimicked *in vitro* and *in vivo* by drugs that elevate cAMP. These studies are the first to implicate cAMP suppression as a critical growth-promoting event downstream of CXCR4 activation. As such, they advance our efforts to improve brain tumor therapy by identifying cAMP elevation as a novel therapeutic strategy.

Materials and Methods

All animals were used in accordance with an established Animal Studies Protocol approved by The Washington University School of Medicine Animal Studies Committee.

Cell Culture and *In vitro* Drug Treatments

Tumor cell lines. Firefly luciferase-expressing U87 glioblastoma multiforme cells and Daoy medulloblastoma cells were a gift of Dr. Andrew Kung (Dana-Farber Cancer Institute, Harvard Medical School, Boston, MA). Additional U87 and Daoy cells were obtained from the American Type Tissue Culture (Manassas, VA). Enhanced green fluorescent protein (EGFP)-luciferase expressing U87 and Daoy cells were generated via lentiviral infection with FUGW-FL as described (16, 17). Briefly, replication-deficient virus was produced by cotransfection of 293T cells with three viral-encoding plasmids using Fugene 6 (Roche, Basel, Switzerland) according to the manufacturer's instructions. The plasmids were (*a*) an expression vector containing transgenes for EGFP and firefly luciferase, (*b*) a plasmid containing vesicular stomatitis virus coat protein for pseudotyping, and (*c*) the Δ packaging vector. Viral particles were collected from 293T cell supernatants and applied to tumor cell cultures. EGFP-expressing cells were sorted and collected by high-speed fluorescence-activated cell sorting.

Note: Supplementary data for this article are available at Cancer Research Online (http://cancerres.aacrjournals.org/).

J.B. Rubin is a scholar of the Child Health Research Center of Excellence in Developmental Biology at Washington University School of Medicine.

Requests for reprints: Joshua B. Rubin, Department of Pediatrics, Division of Pediatric Hematology/Oncology, Washington University School of Medicine, Campus Box 8208, 660 South Euclid Avenue, St. Louis, MO 63110. Phone: 314-286-2790; Fax: 314-286-2892; E-mail: Rubin_J@kids.wustl.edu.

doi:10.1158/0008-5472.CAN-06-2762

Brain tumor cell cultures. Cells were cultured in αMEM (Invitrogen, Carlsbad, CA) supplemented with 10% FCS (Biomedia, Foster City, CA) in the presence of penicillin/streptomycin at 37°C with 5% CO_2.

Primary astrocyte cultures. Primary astrocytes were cultured from 1- to 3-day-old BALB/c mice as described (18). The cortices were triturated into single cells in minimal essential medium (Invitrogen) containing 10% FCS and then plated onto poly-D-lysine coated 75-cm^2 T flasks (0.5 cortical hemisphere/flask) for 10 to 14 days. Astrocytes were purified by first removing nonadherent cells through vigorous shaking of T flasks overnight and then isolating the remaining adherent astrocytes with 0.1% trypsin.

Primary granule neuron cultures. Primary cultures of purified granule precursor cells (GPCs) were prepared from 6-day-old BALB/c mice as described (19). Cerebella were dissected, and meninges were removed. After incubation with 0.1% trypsin (Sigma, St. Louis, MO) in HBSS with 125 units/mL DNase (Sigma), 0.5 mmol/L EDTA for 20 min at 37°C, cells were pelleted and washed thrice with HBSS. The final cell suspension was passed through a 100-μm nylon mesh cell strainer (Falcon, Franklin Lakes, NJ). Cells were diluted to 2×10^6 per mL in DMEM/F12 (Life Technologies, Gaithersburg, MD) supplemented with N2 (Life Technologies), 20 mmol/L KCl, and 36 mmol/L glucose and plated onto poly-D-lysine (20 μg/mL; Sigma)–coated plates.

Growth factor and drug treatment. Following serum starvation for 24 h, astrocytes, granule cells, U87 cells, and Daoy cells were treated with 1 μg/mL CXCL12 (Peprotech, Rocky Hill, NJ), 2.5 ng/mL AMD 3465 (kind gift from Simon Fricker), 200 μmol/L rolipram (Sigma), or 10 μmol/L forskolin (Sigma) as indicated. Daoy and U87 cell growth in culture was measured by trypan blue exclusion after 24 and 48 h of treatment, respectively.

Phosphodiesterase 4A Expression

U87 and Daoy cells were transiently transfected with a plasmid encoding a transgene for the tet-off transactivator alone (kind gift from Dr. Louis Muglia, Washington University School of Medicine, St. Louis, MO), a plasmid containing a transgene for tet-off regulated expression of phosphodiesterase 4A (PDE4A) alone (kind gift from Dr. James Cherry, Boston University, Boston, MA), or a combination of both plasmids, using LipofectAMINE (Invitrogen) according to the manufacturer's instructions. Plasmid DNA (2 μg) was mixed with LipofectAMINE (5 μL) per 35-mm^2 dish. Transfection proceeded for 6 h before exchanging transfection media for αMEM supplemented with 10% FCS.

cAMP Measurement

Cell culture. U87 or Daoy cells were serum-starved for 24 h and treated with CXCL12 (1 μg/mL), rolipram (200 μmol/L), AMD 3465 (2.5 ng/mL), or forskolin (10 μmol/L). Cells were lysed in 0.1 mol/L HCl, and particulate matter was removed by centrifugation at >600 × *g* for 10 min. The supernatants were dried down and resuspended in cAMP assay buffer (Assay Designs, Ann Arbor, MI).

Tumor tissue. EGFP-expressing tumor tissue was removed under direct fluorescence microscopy and frozen in liquid nitrogen. Frozen tissue was weighed and homogenized with 10 volumes of 10% ice-cold trichloroacetic acid and then centrifuged for 10 min at 4,000 rpm to remove precipitate. The supernatant was washed thrice with 8 volumes of water-saturated ether. The aqueous phase was dried down and resuspended in cAMP assay buffer.

Determination of cAMP concentration. Competitive immunoassay for cAMP concentration was done using a Correlated-EIA Enzyme Immunoassay kit (Assay Designs) according to the manufacturer's instructions. Briefly, absorbance at 405 nm was measured, and cAMP concentrations were determined by calculation based on a standard curve. Protein concentrations were measured by colorimetric assay (Bio-Rad, Hercules, CA) according to the manufacturer's directions. cAMP values were normalized to protein for each sample individually. To facilitate comparisons between cell types and experiments, all cAMP data have been normalized to control values in each experiment.

Generation of Xenografts

Tumor cell lines were harvested in mid-logarithmic growth phase and resuspended in PBS. Homozygous NCR nude mice (Taconic Farms, Germantown, NY) were anesthetized with ketamine hydrochloride at 150 mg/kg and xylazine at 12 mg/kg (Phoenix Pharmaceuticals, St. Joseph, MO) via i.p. injection. The cranium was exposed, and a small hole was made with a size 34 inverted cone burr (Roboz, Gaithersburg, MD). Mice were fixed in a stereotactic frame (Stoelting, Wood Dale, IL), and 50,000 cells in 10 μL of PBS were injected through a 27-gauge needle over 2 min at 2 mm lateral and posterior to the bregma and 3 mm below the dura. The incision was closed with Vetbond (3M, St. Paul, MN).

In vivo Drug Treatment

Mice were imaged at least twice after implantation of cells to identify those with equivalent tumor growth rates. Two weeks after tumor cell implantation, cohorts of mice with approximately equivalent tumor bioluminescence were divided into equal control and treatment groups. Animals in AMD 3465 experiments received s.c. osmotic pumps (Alzet, Palo Alto, CA) loaded with 10 mg/mL AMD 3465 in sterile PBS or PBS alone, according to the manufacturer's instructions. The infusion rate was 0.25 μL/h (50 μg/d). For the experiments with rolipram or caffeine, mice in the treatment groups received oral administration of rolipram (5 μg/g/d) or caffeine (100 μg/g/d). The concentration of drug in the water was determined from daily measurements of water consumption by each animal over the course of 7 days. Concentrations were adjusted based on water consumption to provide the prescribed dose.

Bioluminescence Imaging

For bioluminescence imaging of living animals, NCR nude mice bearing i.c. xenografts of firefly luciferase–expressing U87 or Daoy cells were injected i.p. with 150 μg/g D-luciferin (Biosynth, Naperville, IL) in PBS, anesthetized with 2.5% isoflurane, and imaged with a charge-coupled device camera-based bioluminescence imaging system (IVIS 50; Xenogen Corp., Alameda, CA; exposure time = 1-60 s, binning = 8, field of view = 12, f/stop = 1, open filter). Signals were displayed as photons/s/cm^2/sr (20). Regions of interest were defined manually at 95% of the maximum pixel output using Living Image and IgorPro Software (version 2.50), and data were expressed as total photon flux (photons per second; ref. 20). Generally, the first mouse images were obtained 24 h following i.c. inoculation of tumor cells. Data were analyzed and plotted as the ratio of bioluminescence on a given treatment day over bioluminescence on the first day.

Immunohistochemistry

Human brain tumor tissue was retrieved from the pathology files at Washington University School of Medicine. Samples were used in accordance with an Institutional Review Board–approved protocol for human research. Formalin-fixed, paraffin-embedded tissue was processed and analyzed as described (13). CXCR4 was detected with a mouse monoclonal antibody (1 μg/mL; R&D Systems, Minneapolis, MN), and CXCL12 was localized with a rabbit polyclonal antibody (1:66 dilution; Peprotech). Phosphorylated CXCR4 (pCXCR4) was detected using our rabbit polyclonal antibody (1:66 dilution). Immunoreactive complexes were detected using the corresponding secondary biotin-conjugated antibodies augmented by streptavidin/horseradish peroxide and visualized by 3,3′-diaminobenzidine supplied by DAKO (Carpinteria, CA).

Western Blot Analysis

Western blot analysis for protein expression was done by standard procedures exactly as described previously (13). Membranes were incubated with the following polyclonal antibodies: phosphorylated extracellular signal-regulated kinase 1/2 (pErk1/2; 1:1,000), pan Erk1/2 (1:5,000), phosphorylated Akt (pAkt; 1:1,0000), pan Akt (1:5,000), and PDE4 (1:1,000) overnight at 4°C. All blots were stripped and reprobed with antibody directed against β-actin (1:5,000). This was followed by incubation with horseradish peroxidase–conjugated secondary antibody (1:15,000; Bio-Rad). All primary antibodies were from Cell Signaling (Beverly, MA) except antibody to PDE4A (Abcam, Cambridge, MA) and β-actin (Sigma). Quantitation of Western blots was done by densitometry using ImageJ software from the NIH.

Results

pCXCR4 is present in medulloblastoma specimens. In human astrocytoma specimens, advanced histologic grade is correlated

with increased phosphorylation of CXCR4 (13). To determine whether this might be a general feature of central nervous system malignancies, we did a similar analysis of CXCR4 phosphorylation in the primitive neural tumor, medulloblastoma. We evaluated a total of 10 pediatric and adult cases comprising the three major histologic variants of medulloblastoma: desmoplastic, classic, and anaplastic/large cell (21). In agreement with our previous studies of medulloblastoma and glioblastoma (12, 13), all specimens exhibited positive tumor cell staining for CXCR4 (data not shown) and endothelial cell staining for CXCL12 (Supplementary Fig. S1*A*). The presence of both CXCL12 and CXCR4 in tumor specimens was associated with the phosphorylation of CXCR4 (pCXCR4) in 5 of 10 cases (Supplementary Fig. S1*B*; Supplementary Table S1). None of the desmoplastic medulloblastomas contained pCXCR4, whereas two of three classic and three of the four anaplastic large cell specimens did (Supplementary Table S1). Compared with the classic examples, desmoplastic medulloblastomas are associated with a slightly better clinical course, whereas anaplastic/large cell medulloblastomas are considerably more aggressive (21). In this small series, the differences in subtype-specific pCXCR4 staining did not reach statistical significance, but the trend suggests that the level of pCXCR4 may correlate with aggressiveness in medulloblastoma.

CXCL12 growth effects are associated with sustained suppression of cAMP. We investigated whether CXCR4 activation was associated with decreased intracellular cAMP in brain tumor cells, and whether there was enhanced CXCL12-induced cAMP suppression in these neoplastic cells compared with normal cells. To model tumor cell responses, we used U87 glioblastoma and Daoy medulloblastoma cell cultures. Although the true cell of origin for glioblastoma and medulloblastoma is still controversial (22), we used primary cultures of cortical astrocytes and cerebellar GPCs as normal counterparts for glioblastoma and medulloblastoma, respectively (23). When we measured time-dependent changes in intracellular cAMP after application of 1 μg/mL of CXCL12, we found that astrocytic cAMP fluctuated between baseline and 40% of baseline (Fig. 1*A*), whereas in GPCs, there was little to no change in cAMP levels (Fig. 1*B*). The cAMP response in tumor cells was markedly different. cAMP levels rapidly declined in both U87 (Fig. 1*A*) and Daoy (Fig. 1*B*) cells and remained suppressed throughout the experimental period. Area-under-the-curve measurements indicated that in U87 cells, there was a 45% reduction in intracellular cAMP compared with astrocytes (Fig. 1*A*), whereas in Daoy cells, cAMP was reduced by 70% compared with GPCs (Fig. 1*B*).

Differences in cAMP suppression were correlated with differences in CXCL12 growth effects. Although CXCL12 (1 μg/mL) increased U87 (Fig. 1*A*) and Daoy cell (Fig. 1*B*) number by >200%, it tended to decrease astrocyte cell number (Fig. 1*A*) and had no effect on GPC cell number (Fig. 1*B*). In both comparisons, sustained cAMP suppression was correlated with tumor cell growth. This suggested that sustained suppression of cAMP might be a key growth-promoting signal downstream of CXCR4 activation.

CXCL12 growth effects are blocked by elevation of intracellular cAMP. To further evaluate cAMP suppression as the basis for CXCR4-mediated tumor growth, we assessed the ability of drugs that elevate cAMP to block CXCL12-induced growth. cAMP elevation can be pharmacologically achieved by either stimulating adenylyl cyclase or inhibiting cAMP-specific phosphodiesterases. Among the cAMP-specific phosphodiesterases, PDE4 was found to be the predominant isoform in approximately two thirds of

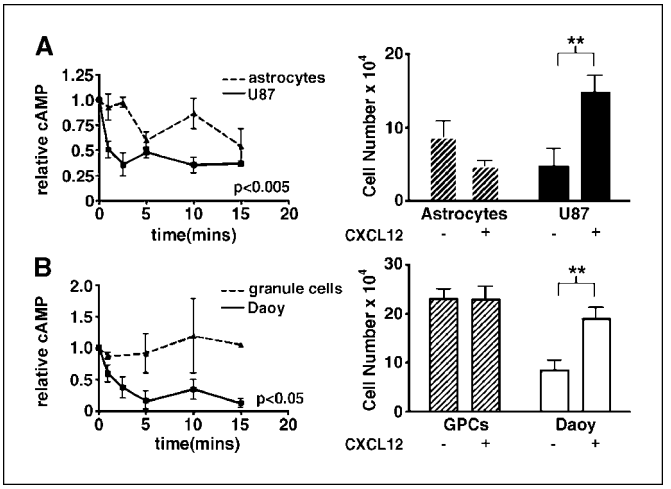

Figure 1. CXCR4-mediated suppression is sustained and associated with growth in brain tumor cells but not in normal counterparts. Primary cultures of (*A*) cortical astrocytes and cultures of U87 glioblastoma cells or (*B*) primary cultures of GPCs and cultures of Daoy medulloblastoma cells were treated with CXCL12 (1 μg/mL), and cAMP was measured by ELISA at various time points as indicated. *Points,* mean of cAMP values normalized to time zero (relative cAMP, $n = 3$); *bars,* SE. $P < 0.005$ (*A*) and $P < 0.05$ (*B*), differences between the curves, two-way ANOVA. In parallel, for primary cultures of astrocytes and U87 cells (*A*), or primary cultures of GPCs and Daoy cells (*B*), the effect of CXCL12 (1 μg/mL) on cell number was measured after 24 h by trypan blue exclusion. *Columns,* mean of representative experiments done in triplicate; *bars,* SE. Each experiment was done a total of three times with similar results. **, $P < 0.005$, two-tailed *t* test.

60 human tumor cell lines (24). PDE4 is highly expressed in the brain (25) and can be specifically inhibited by rolipram. Rolipram is a particularly attractive agent for our purposes as it has been extensively evaluated in human clinical trials as an antidepressant and as an anti-inflammatory agent, including for inflammatory states of the central nervous system, such as multiple sclerosis (26, 27). Thus, in the following studies, we evaluated the effects of adenylyl cyclase activation with forskolin and PDE4 inhibition with rolipram on CXCL12-induced growth responses.

CXCL12 was again observed to increase U87 and Daoy cell number by >2-fold (Fig. 2*A*). Treatment with rolipram had little to no effect on U87 or Daoy cell number alone but completely blocked the growth effects of CXCL12. Forskolin also blocked CXCL12 growth effects in both cell lines but, in addition, was observed to inhibit U87 and Daoy cell growth on its own (Fig. 2*B*). A difference between rolipram and forskolin was also observed for their effects on cAMP. Both drugs blocked CXCL12-induced suppression of cAMP, but only forskolin produced significant increases in cAMP levels (Fig. 2*C*).

AMD 3465 blocks *in vivo* and *in vitro* tumor growth and prevents CXCL12-induced cAMP suppression. We hypothesized that if suppression of cAMP is a key growth-promoting signal downstream of CXCR4 activation, then CXCR4 antagonists must block this suppression. Previously, we evaluated the *in vitro* and *in vivo* antitumor activity of the bicyclam antagonist of CXCR4 activation, AMD 3100 (12). This drug, which functions as a competitive antagonist of CXCL12 binding (28, 29) with partial agonist properties (30, 31), exhibited significant antitumor activity both *in vitro* and *in vivo*. In the present study, we evaluated a newer generation competitive antagonist, AMD 3465. This is a monocyclam with greater affinity for CXCR4 and greater solubility in water (32). CXCL12 again increased U87 and Daoy cell number by

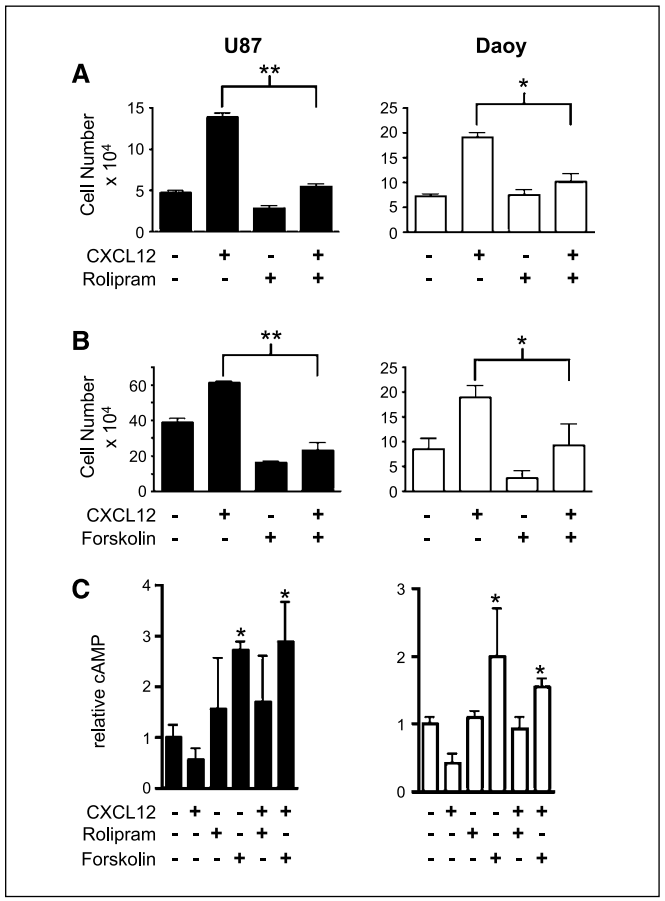

Figure 2. Blocking CXCR4-mediated cAMP suppression blocks CXCL12 growth effects *in vitro*. U87 and Daoy cell cultures were treated with CXCL12 (1 μg/mL) in the presence or absence of (*A*) rolipram (200 μmol/L) or (*B*) forskolin (10 μmol/L). Viable cell number was determined by trypan blue exclusion. *Columns,* mean of representative cell counts; *bars,* SE. Each experiment was done at least three times in triplicate with similar results. *C,* cAMP levels were determined in parallel by ELISA. *Columns,* mean of normalized cAMP values; *bars,* SE. *, $P < 0.05$; **, $P < 0.005$, differences relative to CXCL12 treatment, Dunnett's multiple comparison test ($n = 3$).

>200% (Supplementary Fig. S2*A*). AMD 3465 had no significant effect on cell number alone but completely blocked CXCL12-induced growth in both cell lines.

Similar to studies with AMD 3100 (12), treatment of i.c. xenograft models of medulloblastoma and glioblastoma with AMD 3465 indicated that CXCR4 activation is important to tumor growth *in vivo*. I.c. xenografts of firefly luciferase expressing U87 or Daoy cells were established as described in Materials and Methods. Tumor bearing animals were treated with either continuous s.c. infusion of PBS (control) or AMD 3465 at a dose of 50 μg/d (2.5 mg/kg/d) for 5 weeks. Bioluminescence imaging, which had previously been determined to provide a measure that was linearly related to tumor volume (12), was done weekly, and the means of three separate experiments with five animals per treatment group per experiment were analyzed for antitumor effect. Similar to what we observed for AMD 3100 treatment, AMD 3465 significantly blocked i.c. xenograft growth (Supplementary Fig. S2*B*). U87 GBM xenografts were inhibited by 80%, and Daoy xenografts were inhibited by 85%, compared with controls.

The molecular basis for CXCR4-dependent brain tumor growth is not apparent from the above experiments. Glioblastoma and medulloblastoma typically possess multiple genetic abnormalities that constitutively drive proliferation and survival pathways when assayed *in vitro* (21, 33). We sought to determine which intracellular pathways downstream of CXCR4 activation were most critical to its tumor growth effects. To do this, we investigated which pathways were both activated by CXCL12 and blocked by cotreatment with CXCL12 and AMD 3465, in a manner that correlated with effects on growth. Activation of Erk1/2 and Akt have been implicated in the stimulation of both astrocytoma (34) and medulloblastoma (35, 36) growth. Therefore, we examined Erk1/2 and Akt phosphorylation in Daoy and U87 cells in response to CXCL12 and AMD 3465.

Both CXCL12 and AMD 3465 treatment stimulated the phosphorylation of Erk1/2 in U87 and Daoy cells (Fig. 3*A*; Supplementary Fig. S3*A*). Although AMD 3465 was less potent than CXCL12, these observations still suggest that similar to AMD 3100, AMD 3465 possesses partial agonist activity. Contrary to our observations with AMD 3100 (12), cotreatment of Daoy and U87 cells with CXCL12 and AMD 3465 was also associated with the phosphorylation of Erk1/2. This was particularly striking in the treatment of U87 cells, where cotreatment resulted in a significant increase in Erk1/2 phosphorylation. Neither U87 nor Daoy cells exhibited large increases in Akt phosphorylation in response to CXCL12, AMD 3465, or the two compounds together (Fig. 3; Supplementary Fig. S3). Thus, Erk1/2 is activated under conditions that stimulate growth (CXCL12 alone) and conditions that do not stimulate growth (AMD 3465 alone and cotreatment with CXCL12 and AMD 3465). Together, these data suggest that the activation of Erk1/2 and Akt are not clearly correlated with the growth effects of CXCL12 or the growth-inhibitory effects of AMD 3465.

A clearer relationship between growth and signaling activity was evident, however, in the effects of CXCL12 and AMD 3465 on cAMP

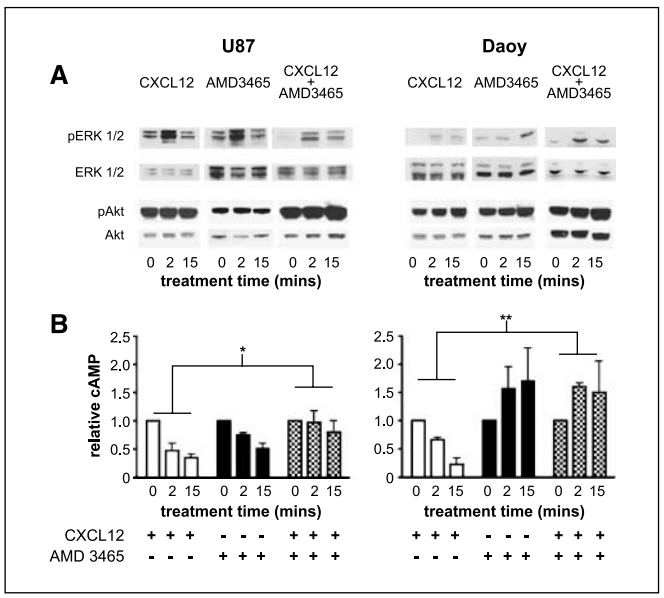

Figure 3. AMD 3465 blocks CXCR4-mediated cAMP suppression. U87 and Daoy cultures were treated with 1 μg/mL CXCL12, 2.5 ng/mL AMD 3465, or both agents together for indicated time points. *A,* phosphorylation of Erk1/2 and Akt was determined by Western blot analysis using pErk1/2- and pAkt-specific antibodies. Total Erk1/2 and total Akt labeling serves as loading controls. *B,* cAMP was determined by ELISA in parallel cultures. *Columns,* mean of cAMP values normalized to time zero (relative cAMP); *bars,* SE. *, $P < 0.05$; **, $P < 0.005$, differences between treatments, two-way ANOVA ($n = 3$).

suppression. As described above, CXCL12 induced rapid declines in cAMP in both cell lines (Fig. 3*B*). AMD 3465 alone had differing effects on U87 and Daoy cells. In U87 cells, there was a trend towards a decrease, whereas in Daoy cells, there was a trend towards an increase, in cAMP in response to AMD 3465. In neither case did these changes reach statistical difference compared with controls. When CXCL12 and AMD 3465 were co-administered, the CXCL12-induced suppression of cAMP was blocked. Thus, cAMP was only significantly suppressed under conditions that stimulated growth (CXCL12 alone). These data support the hypothesis that the suppression of cAMP is a key growth-promoting signal downstream of CXCR4 activation, and that the antitumor effect of AMD 3465 is uniquely dependent upon its ability to block this aspect of CXCR4 signaling.

To confirm that cAMP suppression was a critical downstream event in CXCR4-mediated growth, we transfected U87 (Fig. 4*A*) and Daoy (Fig. 4*B*) cells with a plasmid encoding PDE4A under the control of a tet-off regulatory element alone, or together with a plasmid encoding the tet transactivator. Thus, in the absence of doxycycline, transactivation results in exogenous PDE4A expression and decreases in intracellular cAMP. If suppression of cAMP is a critical growth-promoting event downstream of CXCR4 activation, then expression of PDE4 should mimic the activity of CXCL12. PDE4A expression driven by the transactivator resulted in an increase in PDE4A expression and a decline in intracellular cAMP in both U87 and Daoy cells (Fig. 4). This decrease in intracellular cAMP was associated with an increase in cell growth in culture. In both cell lines, increased phosphodiesterase expression and decreased cAMP was associated with increases in cell number that were comparable with the effect of CXCL12 alone. Under these conditions, there was no additional, significant effect of CXCL12 on cell number or cAMP levels, compared with controls. Moreover, AMD 3465 had no effect on cell number alone or in combination with CXCL12. In contrast, rolipram continued to exert a growth-inhibitory effect. These data further support the hypothesis that the primary growth-promoting activity of CXCL12 is the reduction of intracellular cAMP, and that cAMP suppression is downstream of CXCR4 activation.

Rolipram exhibits significant antitumor activity in i.c. xenograft models of malignant brain tumors. Given the *in vitro* activity of rolipram, we hypothesized that it would exhibit significant antitumor activity *in vivo*. Cohorts of animals with intracranial implants of luciferase-expressing U87 or Daoy xenografts were generated as described in Materials and Methods and treated, beginning 2 weeks after tumor cell injection, with rolipram (5 μg/g/d) delivered in the drinking water versus water alone. Treated animals seemed well throughout the treatment period. Records of individual animal weights indicated that weights were better maintained in the treatment compared with the control group (data not shown). Bioluminescence imaging was done weekly, and the means of three separate experiments with five animals per treatment group per experiment were analyzed for antitumor effects (Fig. 5*A*). Rolipram exhibited significant antitumor activity in both tumor models. Rolipram inhibited U87 xenograft growth by 96% (Fig. 5*B*). This exceeded the growth-inhibitory effect of the CXCR4 antagonist AMD 3465 in the same xenograft system (compare Fig. 5*B* with Supplementary Fig. S2*B*). The effect of rolipram on Daoy xenografts was smaller, producing only a 58% inhibition of growth, a value comparable with the activity of AMD 3465. To assess whether other phosphodiesterase inhibitors might possess similar antitumor activity, we treated i.c. Daoy xenografts with the nonspecific

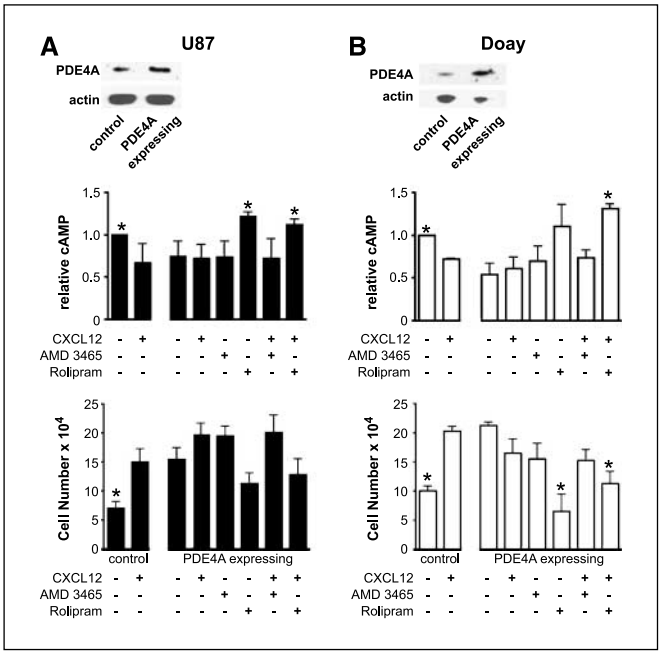

Figure 4. Overexpression of PDE4A abrogates CXCL12 growth effects. U87 (*A*) and Daoy (*B*) cells were transfected with a plasmid encoding PDE4A under control of a tet-off regulatory element (control) or cotransfected with the plasmids encoding PDE4A and the tet-off transactivator (PDE4A expressing). Cotransfection resulted in an increase in PDE4A expression as determined by Western blot analysis. Actin serves as loading control. Cultures were treated with CXCL12 (1 μg/mL), AMD 3465 (2.5 ng/mL), and rolipram (200 μmol/L) as indicated. cAMP was measured by ELISA, and viable cell number was determined by trypan blue exclusion. *Columns,* means of cell counts and normalized cAMP values; *bars,* SE. *, $P < 0.05$; **, $P < 0.005$, differences relative to CXCL12 treatment, Dunnett's multiple comparison test ($n = 3$).

phosphodiesterase inhibitor caffeine (100 μg/g/d). We observed an 85% reduction in tumor growth, an antitumor effect that was greater than rolipram or AMD 3465 (Fig. 5*C*).

To ascertain whether the *in vivo* antitumor effects of rolipram and AMD 3465 were correlated with increases in intratumoral cAMP, we repeated the treatment paradigms with Daoy xenografts that had been engineered to express both EGFP and firefly luciferase. This was done to enable the re-isolation of tumor tissue for extraction of cAMP. After 5 weeks of treatment, tumor tissue was easily visualized *in situ* under direct fluorescence microscopy (Fig. 6*A*). cAMP was extracted from GFP-positive tissue, and cAMP levels were measured by ELISA. The antitumor activity of rolipram and AMD 3465 was associated with a small but significant increase in the amount of cAMP within tumor tissue (Fig. 6*B*). Together, these data strongly support the hypothesis that cAMP suppression is a key growth-promoting event downstream of CXCR4 activation, and that that elevation of tumor cell cAMP has significant anti-brain tumor effect.

Discussion

The expression of pCXCR4 in human brain tumors and the potent anti-xenograft activity of AMD 3100 and AMD 3465 place CXCR4 among the few validated targets for molecular therapy of malignant brain tumors. For CXCR4, epidermal growth factor receptor (37), platelet-derived growth factor receptor (38), and mammalian target of rapamycin (39), abnormal levels of activation are correlated with malignant growth, and correction of this activity in the experimental setting can abrogate growth dysregulation (40).

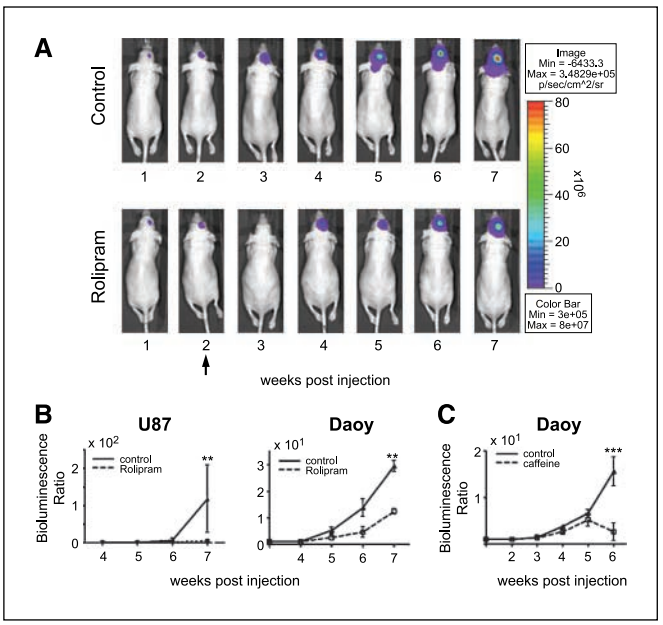

Figure 5. cAMP-elevating drugs block brain tumor growth *in vivo*. *A,* representative weekly bioluminescence images from mice bearing Daoy xenografts from control and oral rolipram (5 μg/g/d) treatment groups. *Arrow,* start of treatment. *B, points,* mean of weekly bioluminescence ratios of U87 and Daoy xenograft control and rolipram treatment group photon flux values over pretreatment values (10 animals per group); *bars,* SE. *C, points,* mean of weekly bioluminescence ratios of Daoy control and caffeine (100 μg/g/d) treatment group photon flux values over pretreatment values (10 animals per treatment group); *bars,* SE. **, $P < 0.005$; ***, $P < 0.0005$, difference between the curves, two-way ANOVA.

The appropriate therapeutic approach for antagonizing CXCR4 remains unclear. Single doses of AMD 3100 have proven useful for the mobilization of bone marrow stem cells before autologous bone marrow transplant (41, 42). Sustained dosing of AMD 3100 over a 10-day period, however, was associated with mild toxicities, and reflective of its effects on bone marrow function, elevations of WBC counts were evident throughout an 18-day follow-up period after cessation of AMD 3100 (43). Whether these toxicities and sustained effects on marrow function would preclude the prolonged delivery of AMD 3100, related analogues, or other CXCR4 antagonists to cancer patients is not known, but the necessity for continued evaluation of this pathway and alternative antagonist approaches is clear.

CXCR4 is a G_i-coupled GPCR, and, in these experiments, the suppression of intracellular cAMP seemed to be the key event in mediating CXCR4-dependent growth effects. This was apparent in the differences between CXCL12-induced cAMP suppression and growth in U87 cells compared with astrocytes and Daoy cells compared with GPCs. The importance of cAMP suppression to growth was also evident in the ability of adenylyl cyclase activation with forskolin and PDE4 inhibition with rolipram to elevate intracellular cAMP and block CXCL12-induced tumor cell growth. The ability of PDE4A overexpression to drive increased growth in a manner that was no longer regulated by CXCL12 and no longer sensitive to AMD 3465 places cAMP suppression downstream of CXCR4 activation in stimulating tumor cell growth. Moreover, the induction of Erk1/2 phosphorylation upon cotreatment of tumor cells with CXCL12 and AMD 3465 indicates that cAMP suppression, and not Erk1/2 phosphorylation, is correlated with CXCL12 growth effects. The preserved antitumor effect of rolipram against phosphodiesterase-overexpressing tumor cells further confirms the importance of cAMP to growth regulation, consistent with earlier studies that suggested brain tumor grade was inversely related to adenylyl cyclase activity and intracellular levels of cAMP (1, 2).

In our prior studies, the magnitude of the antitumor effect of the CXCR4 antagonist AMD 3100 was best correlated with its proapoptotic activity (12). Thus, it will be important to identify cAMP-regulated mediators of survival. Targeting cAMP and/or these downstream targets of cAMP might allow for greater specificity in cancer treatment. The role of CXCR4 in maintaining stem cell pools in the bone marrow (42, 44, 45) and in regulating lymphocyte trafficking (46) is dependent upon CXCR4-mediated chemotactic effects. This has previously been shown to be a function of CXCR4-mediated activation of Erk1/2 (47), p38 mitogen-activated protein kinase (48), and Akt (49). There are no observations to suggest that cAMP suppression is necessary for CXCL12-induced chemotaxis. This might therefore provide a differential target by which the disruption of CXCR4-mediated survival would not interfere with CXCR4-mediated chemotaxis.

The smaller effect of rolipram on Daoy compared with U87 xenografts may be due to the presence of cAMP-independent growth-promoting pathways downstream of CXCR4 in Daoy cells, or there being resistance mechanisms to rolipram in Daoy cells. cAMP levels are tightly regulated and sustained elevations, like those that arise with phosphodiesterase inhibition, can induce regulatory pathways that restore cAMP to baseline levels. This commonly involves transcriptional regulation of phosphodiesterase expression (50). Alternate phosphodiesterase expression as the basis for the smaller response of Daoy cells to rolipram was supported by the activity of caffeine, a nonspecific phosphodiesterase inhibitor.

The significance of identifying cAMP suppression as the mediator of CXCR4 growth effects and rolipram as an antitumor agent lies in the clinical applicability of PDE4 inhibitors. This class of drugs, including, theophylline, AirFlo, and roflumilast, have established applications in the treatment of asthma and chronic

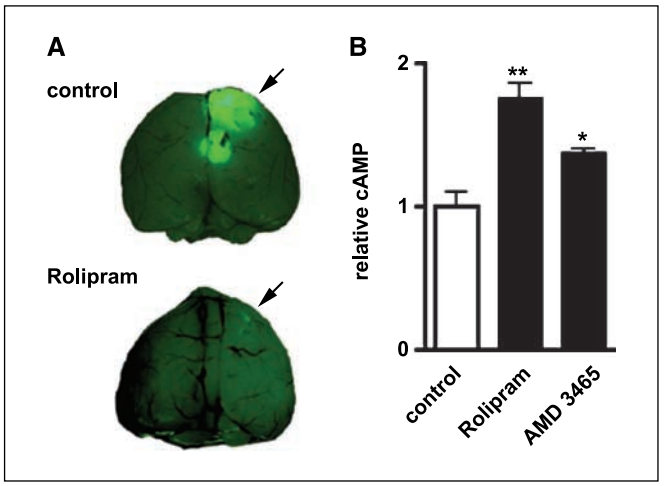

Figure 6. Rolipram elevates intratumoral cAMP *in vivo*. *A,* representative mice from U87 control and oral rolipram (5 μg/g/d) treatment groups showing tumor localization via fluorescence. *B,* cAMP was extracted from tumor tissue and measured by ELISA. *Columns,* mean of determinations from three separate animals per treatment group; *bars,* SE. *, $P < 0.05$; **, $P < 0.005$, differences relative to control, Dunnett's multiple comparison test.

obstructive pulmonary disease (51) and as anti-inflammatory agents (27). Rolipram was originally developed as an antidepressant and antidementia medication (26). It crosses an intact blood-brain barrier and may therefore have an additional advantage in the treatment of brain tumors. The potential for resistance might be addressed through the use of combined PDE3 and PDE4A inhibitors, such as zardaverine. Although caffeine exhibited significant anti-xenograft activity and has been shown to enhance cytotoxicity *in vitro* (52), it is less likely to be useful as a clinical agent in the treatment of brain tumors. Addition of pentoxiphyllin, a methylxanthine related to caffeine, to chemotherapy and radiation therapy for patients with malignant gliomas was evaluated in a clinical trial that was terminated due to excessive toxicity, including decreased consciousness and increased seizure activity (53). Therefore, renewed evaluation of specific phosphodiesterase inhibitors, like rolipram, for the treatment of brain and other cancers is warranted.

The importance of targeting CXCR4 in the treatment of brain and other cancers is clear. However, the optimal mode of CXCR4 antagonism is not yet known. These studies suggest that targeting the downstream suppression of cAMP may be efficacious and tractable. The clinical availability of drugs that elevate cAMP and will cross the blood-brain barrier makes this an especially attractive treatment approach.

Acknowledgments

Received 7/26/2006; revised 10/4/2006; accepted 10/26/2006.

Grant support: Hope Street Kids (J.B. Rubin), Edward Mallinckrodt Jr. Foundation (J.B. Rubin), Children's Brain Tumor Foundation (J.B. Rubin), and NIH grant P50 CA94056 (D. Piwnica-Worms).

The costs of publication of this article were defrayed in part by the payment of page charges. This article must therefore be hereby marked *advertisement* in accordance with 18 U.S.C. Section 1734 solely to indicate this fact.

We thank Drs. Alan Schwartz, Jonathan Gitlin, Louis Muglia, and Robyn Klein for critical reading of the article and Drs. Gary Bridger and Simon Fricker (AnorMed, Langley, British Columbia, Canada) for AMD 3465 and helpful discussions.

References

1. Furman MA, Shulman K. Cyclic AMP and adenyl cyclase in brain tumors. J Neurosurg 1977;46:477–83.
2. Racagni G, Pezzotta S, Giordana MT, et al. Cyclic nucleotides in experimental and human brain tumors. J Neurooncol 1983;1:61–7.
3. Magnaldo I, Pouyssegur, Paris S. Cyclic AMP inhibits mitogen-induced DNA synthesis in hamster fibroblasts, regardless of the signalling pathway involved. FEBS Lett 1989;245:65–9.
4. Sewing A, Burger C, Brusselbach S, Schalk C, Lucibello FC, Muller R. Human cyclin D1 encodes a labile nuclear protein whose synthesis is directly induced by growth factors and suppressed by cyclic AMP. J Cell Sci 1993; 104:545–55.
5. Balmanno K, Millar T, McMahon M, Cook SJ. DeltaRaf-1:ER* bypasses the cyclic AMP block of extracellular signal-regulated kinase 1 and 2 activation but not CDK2 activation or cell cycle reentry. Mol Cell Biol 2003;23: 9303–17.
6. Kato JY, Matsuoka M, Polyak K, Massague J, Sherr CJ. Cyclic AMP-induced G_1 phase arrest mediated by an inhibitor (p27Kip1) of cyclin-dependent kinase 4 activation. Cell 1994;79:487–96.
7. Reginato MJ, Mills KR, Paulus JK, et al. Integrins and EGFR coordinately regulate the pro-apoptotic protein Bim to prevent anoikis. Nat Cell Biol 2003;5:733–40.
8. Li H, Kolluri SK, Gu J, et al. Cytochrome *c* release and apoptosis induced by mitochondrial targeting of nuclear orphan receptor TR3. Science 2000;289:1159–64.
9. Harada H, Becknell B, Wilm M, et al. Phosphorylation and inactivation of BAD by mitochondria-anchored protein kinase A. Mol Cell 1999;3:413–22.
10. Rempel SA, Dudas S, Ge S, Gutierrez JA. Identification and localization of the cytokine SDF1 and its receptor, CXC chemokine receptor 4, to regions of necrosis and angiogenesis in human glioblastoma. Clin Cancer Res 2000;6:102–11.
11. Sehgal A, Keener C, Boynton AL, Warrick J, Murphy GP. CXCR-4, a chemokine receptor, is overexpressed in and required for proliferation of glioblastoma tumor cells. J Surg Oncol 1998;69:99–104.
12. Rubin JB, Kung AL, Klein RS, et al. A small-molecule antagonist of CXCR4 inhibits intracranial growth of primary brain tumors. Proc Natl Acad Sci U S A 2003; 100:13513–8.
13. Woerner BM, Warrington NM, Kung AL, Perry A, Rubin JB. Widespread CXCR4 activation in astrocytomas revealed by phospho-CXCR4-specific antibodies. Cancer Res 2005;65:11392–9.
14. Ehtesham M, Winston JA, Kabos P, Thompson RC. CXCR4 expression mediates glioma cell invasiveness. Oncogene 2006;25:2801–6.
15. Marinissen MJ, Gutkind JS. G-protein-coupled receptors and signaling networks: emerging paradigms. Trends Pharmacol Sci 2001;22:368–76.
16. Smith MC, Luker KE, Garbow JR, et al. CXCR4 regulates growth of both primary and metastatic breast cancer. Cancer Res 2004;64:8604–12.
17. Lois C, Hong EJ, Pease S, Brown EJ, Baltimore D. Germline transmission and tissue-specific expression of transgenes delivered by lentiviral vectors. Science 2002; 295:868–72.
18. Dasgupta B, Dugan LL, Gutmann DH. The neurofibromatosis 1 gene product neurofibromin regulates pituitary adenylate cyclase-activating polypeptide-mediated signaling in astrocytes. J Neurosci 2003;23: 8949–54.
19. Rubin JB, Choi Y, Segal RA. Cerebellar proteoglycans regulate sonic hedgehog responses during development. Development 2002;129:2223–32.
20. Gross S, Piwnica-Worms D. Real-time imaging of ligand-induced IKK activation in intact cells and in living mice. Nat Methods 2005;2:607–14.
21. Giangaspero F, Bigner SH, Kleihues, et al. Medulloblastoma. In: Kleihues PC, Cavenee WK, editors. World Health Organization classification of tumours: pathology and genetics of tumours of the nervous system. Lyon: IARC Press; 2000.
22. Sanai N, Alvarez-Buylla A, Berger MS. Neural stem cells and the origin of gliomas. N Engl J Med 2005;353: 811–22.
23. Oliver TG, Read TA, Kessler JD, et al. Loss of patched and disruption of granule cell development in a pre-neoplastic stage of medulloblastoma. Development 2005;132:2425–39.
24. Marko D, Pahlke G, Merz KH, Eisenbrand G. Cyclic 3′,5′-nucleotide phosphodiesterases: potential targets for anticancer therapy. Chem Res Toxicol 2000;13:944–8.
25. DaSilva JN, Lourenco CM, Meyer JH, Hussey D, Potter WZ, Houle S. Imaging cAMP-specific phosphodiesterase-4 in human brain with R-[11C]rolipram and positron emission tomography. Eur J Nucl Med Mol Imaging 2002;29:1680–3.
26. Wachtel H, Schneider HH. Rolipram, a novel antidepressant drug, reverses the hypothermia and hypokinesia of monoamine-depleted mice by an action beyond postsynaptic monoamine receptors. Neuropharmacology 1986;25:1119–26.
27. Dyke HJ, Montana JG. Update on the therapeutic potential of PDE4 inhibitors. Expert Opin Investig Drugs 2002;11:1–13.
28. De Clercq E. The bicyclam AMD3100 story. Nat Rev Drug Discov 2003;2:581–7.
29. Bridger GJ, Skerlj RT, Padmanabhan S, et al. Synthesis and structure-activity relationships of phenylenebis (methylene)-linked bis-azamacrocycles that inhibit HIV-1 and HIV-2 replication by antagonism of the chemokine receptor CXCR4. J Med Chem 1999;42:3971–81.
30. Zhang WB, Navenot JM, Haribabu B, et al. A point mutation that confers constitutive activity to CXCR4 reveals that T140 is an inverse agonist and that AMD3100 and ALX40–4C are weak partial agonists. J Biol Chem 2002;277:24515–21.
31. Trent JO, Wang ZX, Murray JL, et al. Lipid bilayer simulations of CXCR4 with inverse agonists and weak partial agonists. J Biol Chem 2003;278:47136–44.
32. Hatse S, Princen K, De Clercq E, et al. AMD3465, a monomacrocyclic CXCR4 antagonist and potent HIV entry inhibitor. Biochem Pharmacol 2005;70:752–61.
33. Kleihues P, Burger PC, Collins, et al. Glioblastoma. In: Kleihues PC, Cavenee WK, editors. World Health Organization classification of tumours: pathology and genetics of tumours of the nervous system. Lyon: IARC Press; 2000.
34. Pelloski CE, Lin E, Zhang L, et al. Prognostic associations of activated mitogen-activated protein kinase and Akt pathways in glioblastoma. Clin Cancer Res 2006;12:3935–41.
35. MacDonald TJ, Brown KM, LaFleur B, et al. Expression profiling of medulloblastoma: PDGFRA and the RAS/MAPK pathway as therapeutic targets for metastatic disease. Nat Genet 2001;29:143–52.
36. Hartmann W, Digon-Sontgerath B, Koch A, et al. Phosphatidylinositol 3′-kinase/AKT signaling is activated in medulloblastoma cell proliferation and is associated with reduced expression of PTEN. Clin Cancer Res 2006;12:3019–27.
37. Lassman AB, Abrey LE, Gilbert MR. Response of glioblastomas to EGFR kinase inhibitors. N Engl J Med 2006;354:525–6; author reply -6.
38. Kilic T, Alberta JA, Zdunek PR, et al. Intracranial inhibition of platelet-derived growth factor-mediated glioblastoma cell growth by an orally active kinase inhibitor of the 2-phenylaminopyrimidine class. Cancer Res 2000;60:5143–50.
39. Dasgupta B, Yi Y, Chen DY, Weber JD, Gutmann DH. Proteomic analysis reveals hyperactivation of the mammalian target of rapamycin pathway in neurofibromatosis 1-associated human and mouse brain tumors. Cancer Res 2005;65:2755–60.
40. Kondo Y, Hollingsworth EF, Kondo S. Molecular targeting for malignant gliomas [review]. Int J Oncol 2004;24:1101–9.
41. Devine SM, Flomenberg N, Vesole DH, et al. Rapid mobilization of $CD34^+$ cells following administration of the CXCR4 antagonist AMD3100 to patients with multiple myeloma and non-Hodgkin's lymphoma. J Clin Oncol 2004;22:1095–102.
42. Broxmeyer HE, Orschell CM, Clapp DW, et al. Rapid mobilization of murine and human hematopoietic stem

and progenitor cells with AMD3100, a CXCR4 antagonist. J Exp Med 2005;201:1307–18.
43. Hendrix CW, Collier AC, Lederman MM, et al. Safety, pharmacokinetics, and antiviral activity of AMD3100, a selective CXCR4 receptor inhibitor, in HIV-1 infection. J Acquir Immune Defic Syndr 2004;37:1253–62.
44. Ma Q, Jones D, Springer TA. The chemokine receptor CXCR4 is required for the retention of B lineage and granulocytic precursors within the bone marrow microenvironment. Immunity 1999;10:463–71.
45. Basu S, Broxmeyer HE. Transforming growth factor-{beta}1 modulates responses of $CD34^+$ cord blood cells to stromal cell-derived factor-1/CXCL12. Blood 2005;106:485–93.
46. Bleul CC, Schultze JL, Springer TA. B lymphocyte chemotaxis regulated in association with microanatomic localization, differentiation state, and B cell receptor engagement. J Exp Med 1998;187:753–62.
47. Floridi F, Trettel F, Di Bartolomeo S, Ciotti MT, Limatola C. Signalling pathways involved in the chemotactic activity of CXCL12 in cultured rat cerebellar neurons and CHP100 neuroepithelioma cells. J Neuroimmunol 2003;135:38–46.
48. Sun Y, Cheng Z, Ma L, Pei G. Beta-arrestin2 is critically involved in CXCR4-mediated chemotaxis, and this is mediated by its enhancement of p38 MAPK activation. J Biol Chem 2002;277:49212–9.
49. Vicente-Manzanares M, Rey M, Jones DR, et al. Involvement of phosphatidylinositol 3-kinase in stromal cell-derived factor-1 alpha-induced lymphocyte polarization and chemotaxis. J Immunol 1999;163:4001–12.
50. Persani L, Lania A, Alberti L, et al. Induction of specific phosphodiesterase isoforms by constitutive activation of the cAMP pathway in autonomous thyroid adenomas. J Clin Endocrinol Metab 2000;85:2872–8.
51. Cowan C. Roflumilast for asthma and chronic obstructive pulmonary disease. Issues Emerg Health Technol 2005:1–4.
52. Janss AJ, Levow C, Bernhard EJ, et al. Caffeine and staurosporine enhance the cytotoxicity of cisplatin and camptothecin in human brain tumor cell lines. Exp Cell Res 1998;243:29–38.
53. Stewart DJ, Dahrouge S, Agboola O, Girard A. Cranial radiation and concomitant cisplatin and mitomycin-C plus resistance modulators for malignant gliomas. J Neurooncol 1997;32:161–8.

Blocking CXCR4-Mediated Cyclic AMP Suppression Inhibits Brain Tumor Growth *In vivo*

Lihua Yang, Erin Jackson, B. Mark Woerner, et al.

Cancer Res 2007;67:651-658.